

# Crystallization of PP in PP/SEBS Blends and Its Correlation with Tensile Properties

A. K. GUPTA and S. N. PURWAR, *Centre for Materials Science and Technology, Indian Institute of Technology, New Delhi—110 016, India*

## Synopsis

Crystallization of polypropylene (PP) in the blends of PP with styrene-ethylene butylene-styrene triblock copolymer (SEBS) is studied through differential thermal analysis (DTA) and X-ray diffraction measurements. Analysis of crystallization exotherm peaks in terms of crystallization nucleation and growth rates, crystallite size distribution, and crystallinity revealed differences in the morphology of PP component in the blend in the different regions of blend composition. Crystallinity determined by X-ray diffraction and DTA showed identical variations with blend composition. Variations in tensile properties of these blends with blend composition are also reported. Correlations of the various tensile properties with the crystallization parameters, viz., the crystallinity and crystallite size distribution, are presented, which confirm the influence of crystallization of PP component on the tensile properties of these blends.

## INTRODUCTION

It has been shown<sup>1</sup> that blending of polypropylene (PP) with high density polyethylene (HDPE) or reinforcement with short glass fiber affects the crystallization and morphology of PP. An understanding of the crystallization behavior of PP is of great importance to explain the mechanical properties of polyblends and composites involving PP as the major component.

Blends of PP with various other polymers have been reported<sup>2-5</sup> to show improvements in mechanical and rheological properties suited to many applications. SEBS (styrene-ethylene butylene-styrene) triblock copolymer, obtained by hydrogenation of the butadiene sequence, is a recently developed thermoplastic elastomer.

Blends of SEBS with HDPE and polystyrene (PS) and the development of thermoplastic interpenetrating polymer networks (IPN) with SEBS were recently reported.<sup>6</sup> Lindsey, Paul, and Barlow<sup>7</sup> found that addition of SEBS to the binary HDPE-PS blends improved the ductility, toughness, and various mechanical properties but lowered the strength and modulus. In the case of thermoplastic IPN's, Siegfried, Thomas, and Sperling<sup>6</sup> developed the two types of thermoplastic IPN's (chemically blended and mechanically blended) with styrene, methacrylic acid, and isoprene monomers. They<sup>6</sup> found a dual phase continuity after ionomer formation in both types of these IPNs, while the melt viscosity was lower in the chemically blended IPN than the mechanically blended one. Blends of SEBS with PP, reported<sup>8</sup> recently by us, have shown considerable improvement in the melt rheological properties of PP, favorable from the point of view of processing.

In this paper we present a study of crystallization of PP in the blend of PP and SEBS, with SEBS content varying from 5 to 25 wt %. The crystallization be-

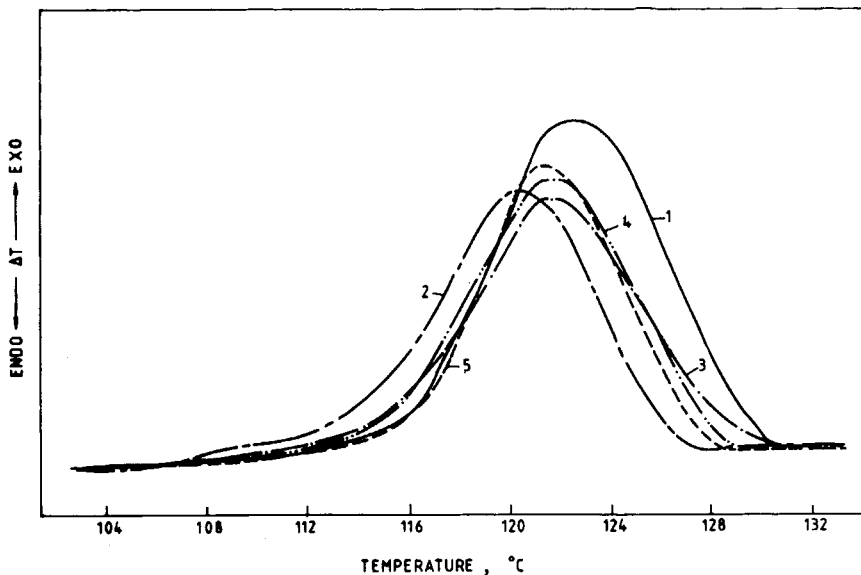


Fig. 1. DTA thermograms of PP and PP/SEBS blends of varying blend compositions: (1) PP; (2) 5% SEBS; (3) 10% SEBS; (4) 15% SEBS; (5) 25% SEBS.

havior and the degree of crystallinity are determined through the differential thermal analysis (DTA) and X-ray diffraction measurements. Use of thermal analysis techniques (DTA or DSC) for the study of crystallization kinetics of PP is illustrated in the literature<sup>1,9</sup> DTA or DSC thermogram of PP shows well-developed crystallization exotherm peak when recorded during the cooling cycle in a wide range of cooling rates. Changes in the shape and position of the exotherm are related to the changes in nucleation and growth rates as well as in the overall crystallinity and distribution of crystallite (or spherulite) size. Changes in the crystallization exotherm of PP on blending with SEBS with varying fraction of SEBS are presented along with the accompanying changes in X-ray diffraction and the mechanical properties.

## EXPERIMENTAL

**Materials.** Isotactic polypropylene (PP), Koylene M 3030, of Indian Petrochemical Corporation Ltd. (melt flow index 3.0) and styrene-ethylene butylene-styrene block copolymer (SEBS), Kraton G-1652 of Shell Chemical Company (details of this sample described elsewhere<sup>6,7</sup>) were used.

**Preparation of Blends.** Blends of PP and SEBS with blend composition 5–25 wt % SEBS were prepared by melt blending method in a single screw extruder (Betol BM1820) at screw rpm of 40, keeping the temperature profile 200°C (first zone), 210°C (second zone), 220°C (third zone), and 220°C (die zone). The thick continuous strands of the blends obtained after extrusion mixing process were cut into granules and then the granules were ground to 25-mesh size, washed with methanol, and dried under vacuum at 60°C. These were then injection-molded to prepare the dumbbell shaped samples (ASTM-D-638 Type 1) for tensile testing. DTA and X-ray diffraction measurements were done on ground powder of the blends. The unblended PP samples were also processed through

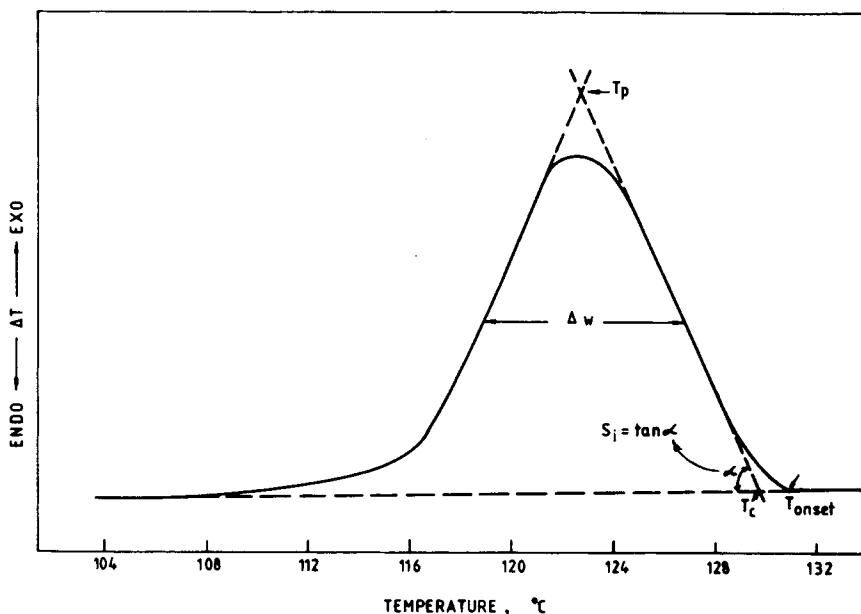


Fig. 2. Schematic representation of the method of determination of the various parameters from DTA crystallization exotherm peak.

identical conditions of extrusion, grinding, and molding, as the blend sample before testing.

**Measurements.** DTA measurements were done on a Stanton Redcroft DTA-671 differential thermal analyzer, using alumina as the reference material. The samples were first heated to 180°C (i.e., 20°C above the melting temperature of PP) and were kept at that temperature for 5 min so as to eliminate the effect of a previous history of crystallization. Thermograms were recorded during the cooling cycle at constant cooling rate 5°C/min, at identical settings of the instrument for all the samples. The sample size used was 10 mg, and measurements were done on at least three samples of each blend composition to ascertain the reproducibility of the results.

X-ray diffraction measurements were done on Philips Norelco X-ray diffraction equipment provided with a scintillation counter and recorder. Radial scans of intensity ( $I$ ) vs. diffraction angle ( $2\theta$ ) were recorded in the range 8°–50° of  $2\theta$  using  $\text{CuK}\alpha$  radiation. Diffractograms of all the samples were recorded at identical settings of the instrument. Reproducibility of the diffractograms was checked through the measurements on at least two samples in all cases.

Tensile properties were measured on an Instron universal testing machine (Model 1121) at constant strain rate 5 cm/min keeping the initial gauge length 6.5 cm. Five samples were tested in each case, and the deviation of data around the mean value was less than 10%.

## RESULTS AND DISCUSSION

### Differential Thermal Analysis

DTA thermograms recorded during the cooling cycle showed quite prominent crystallization exotherm peak of PP in all the blend samples as well as the un-

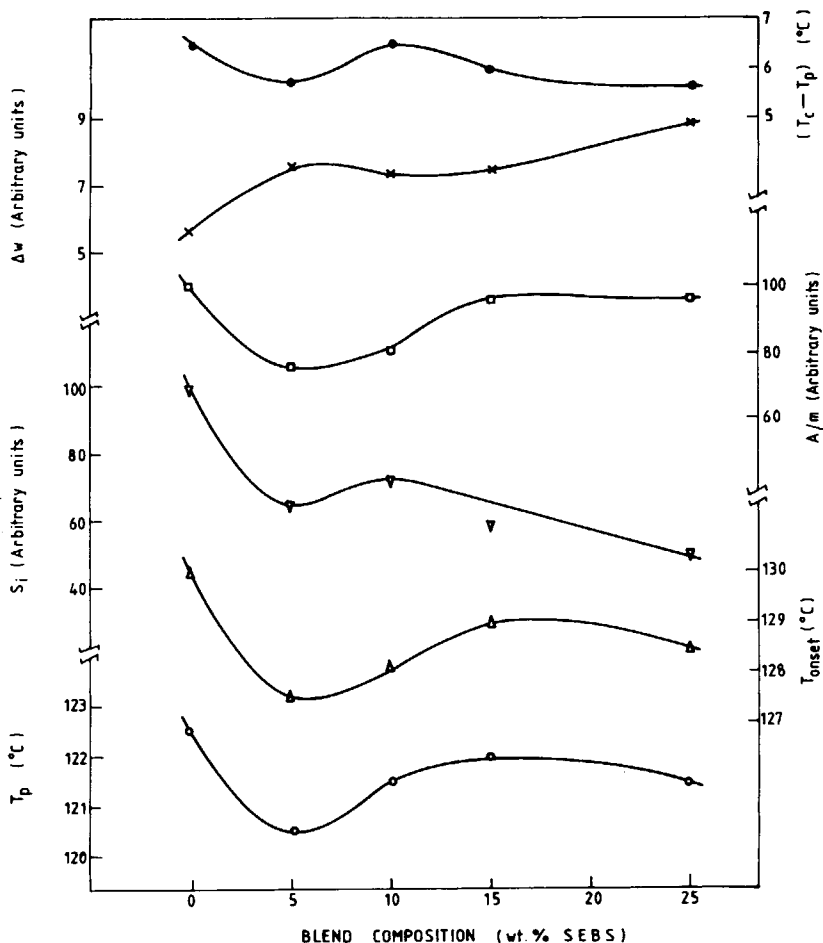


Fig. 3. Variation of the various crystallization parameters with blend composition.

blended PP. These exotherms are presented in Figure 1 for all the samples at the same temperature scale for comparison. These exotherm peaks are situated around  $120 \pm 2^\circ\text{C}$ , which is slightly higher (by about  $10^\circ\text{C}$ ) than the peak temperature of our previously reported<sup>1</sup> DSC exotherms of PP of a different origin. As is clearly seen from Figure 1, the exotherm peak in the PP/SEBS blends occurs at lower temperatures relative to that of unblended PP. Differences in these exotherms are also found in terms of the following quantities, which are known to be related to the crystallization parameters. These quantities, also used by other authors,<sup>1,9</sup> are defined below and illustrated in Figure 2.

(i) The peak temperature of the crystallization exotherm,  $T_p$ , determined as the point of intersection of the tangents at the two sides of the exotherm.

(ii) The temperature of onset of crystallization,  $T_{onset}$ , which is the temperature where the thermogram initially departs from the baseline on the high temperature side of the exotherm.

(iii) Initial slope of the exotherm,  $S_i$ , which is the slope of the high temperature side of the exotherm.

(iv) The quantity  $(T_c - T_p)$ , where  $T_c$  is the temperature at the intercept of the tangents at the baseline and the high temperature side of the exotherm.

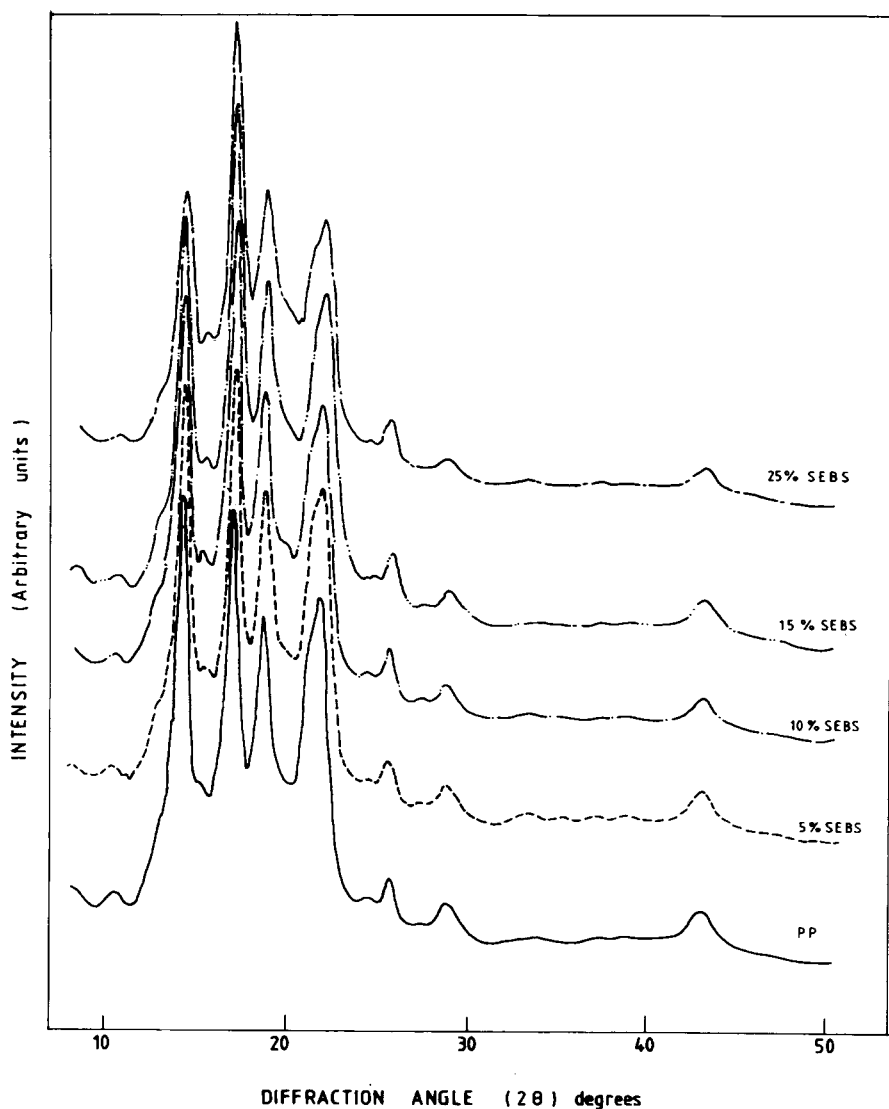


Fig. 4. X-ray diffractograms of PP and the PP/SEBS blends of varying composition.

(v) The quantity  $A/m$ , which is the area under the exotherm divided by the mass of PP component in the sample.

(vi) The width at half-height of the exotherm peak,  $\Delta w$ , determined after normalization of the peak to constant mass of PP component in the sample.

Peak temperature  $T_p$  of exothermic peak is a function of cooling rate and is a measure of supercooling. Decrease in peak temperature implies an increase in supercooling. It has been shown<sup>9,10</sup> that increase in rate of nucleation by addition of nucleating agent or by any other means increased the peak temperature (i.e., reduced the supercooling) of the crystallization exotherm of PP.  $T_{\text{onset}}$  may have similar significance as  $T_p$ , except that their interrelationship is inherently dependent through the parameter  $S_i$ , which may differ from sample to sample. The quantity  $S_i$  is indicative of the rate of nucleation. It has been shown<sup>9</sup> that addition of nucleating agents increased the initial slope  $S_i$  of the

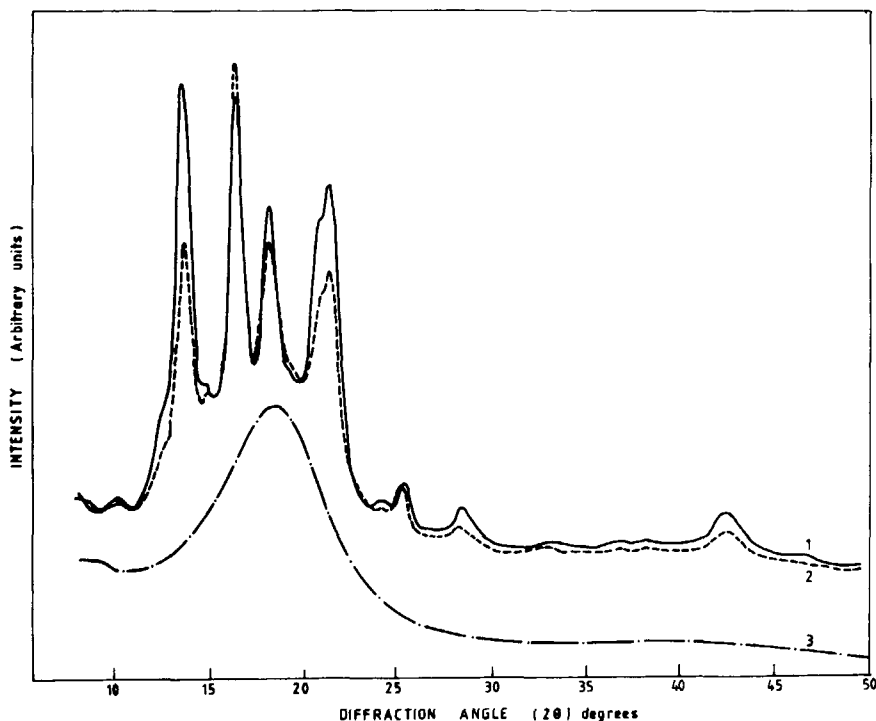


Fig. 5. Comparison of the X-ray diffractograms of PP and the blend sample with highest SEBS content *vis-à-vis* the diffractogram of SEBS. (1) PP; (2) 25% SEBS blend; (3) SEBS.

crystallization exotherm of PP. The parameter  $(T_c - T_p)$  is a measure of the overall rate of crystallization<sup>9</sup>; the smaller the  $(T_c - T_p)$ , the greater the rate of crystallization.  $A/m$  is a quantity proportional to the heat of crystallization of the given sample and thus to its degree of crystallinity.<sup>1</sup> Since the measurements on all the samples were done under identical settings of the instrument, the variations of  $A/m$  may be taken to represent the variations of crystallinity in these samples. The peak width at half-height,  $\Delta w$ , is a measure of the crystallite size distribution<sup>1</sup>; the smaller the  $\Delta w$ , the narrower the size distribution of the crystallites.

$T_p$ ,  $T_{\text{onset}}$ ,  $S_i$ ,  $(T_c - T_p)$ , and  $A/m$  decrease with increasing SEBS content in a manner shown in Figure 3, showing minima around 5% SEBS. On the other hand,  $\Delta w$  increases with increasing SEBS content, showing a rather rapid increase in the region 0 to 5% SEBS, followed by inappreciable increase in the region from 5% to 15% SEBS and a moderate increase above 15% SEBS. Let us denote these three regions of blend composition as regions 1, 2, and 3 comprising of 0–5%, 5–15%, and 15–25% SEBS content, respectively.

These results indicate that:

(1) In region 1 of the blend composition, blending with SEBS decreases the rate of nucleation and growth of crystallization and produces a lower degree of crystallinity of PP in the blend. A slow rate of nucleation may cause the formation of larger spherulites, while the formation of some smaller spherulites may also take place, owing to the slow rate of growth of crystallization. The increase of crystallite size distribution parameter ( $\Delta w$ ) in this region supports this morphological description of PP phase of the blend.

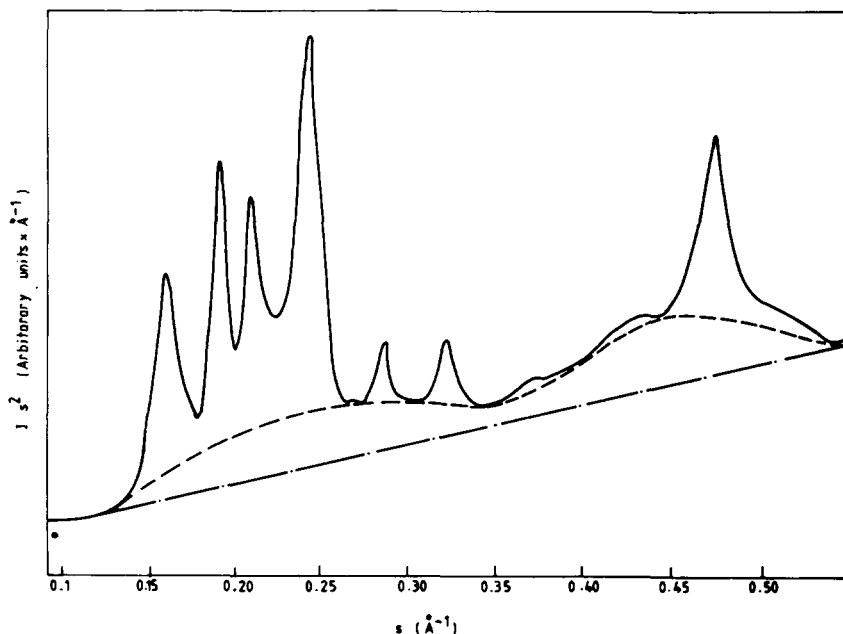


Fig. 6.  $I s^2$  vs.  $s$  plot of PP with baseline and amorphous scattering curve drawn in accordance with that suggested by Sotton et al.<sup>13</sup>

(2) In region 2 of the blend composition, the nucleation and growth rates and the crystallinity increase with increasing SEBS content. Hence a large number of nuclei will be created which may not get sufficient time to grow into large spherulites due to the rapid growth rate. Thus the structure in this case will have a large number of small spherulites. The observed inappreciable change in crystallite size distribution parameter ( $\Delta w$ ) in this region clearly supports this morphological description.

(3) In region 3 of the blend composition, the rates of nucleation and growth of crystallization decrease with increasing SEBS content and the crystallinity also decreases. The rates of decrease of these quantities are somewhat slower than those in the region 1. Distribution of spherulite size also increases in this region, which suggests a somewhat similar morphological description in this region as in the region 1.

### X-Ray Diffraction

X-ray diffractograms of these samples, the intensity ( $I$ ) vs. diffraction angle ( $2\theta$ ) curves, are shown in Figure 4. Diffraction pattern of PP shows several diffraction maxima, of which the four occurring at  $2\theta$  values  $14^\circ$ ,  $17^\circ$ ,  $18.5^\circ$ , and  $21.7^\circ$  are very intense; the last one of these is apparently a doublet. Similar characteristic peaks of crystalline structure of isotactic polypropylene have been reported by Natta and Corradini.<sup>11</sup> Diffraction patterns of the PP/SEBS blend show all the characteristic peaks of PP and no other additional peak, implying that PP is the only crystallizable component in this two phase blend. These diffraction peaks are quite intense for all the blend compositions, indicating sufficiently grown crystallinity of PP in these blends in the studied range of blend composition.

TABLE I  
Values of Various Crystallization Parameters of PP Components in PP/SEBS Blends from DTA Thermograms and X-Ray Diffraction

Sample	$T_p$ (°C)	$T_{onset}$ (°C)	$S_i$ (arbitrary units)	$T_c - T_p$ (°C)	$A/m$ (arbitrary units)	$\Delta w$ (arbitrary units)	$(X_c)_{app}$
PP	122.5	130.0	100	6.5	100	5.6	0.65
PP/SEBS (5%)	120.5	127.5	65	5.7	76	7.6	0.58
PP/SEBS (10%)	121.5	128.0	73	6.5	80	7.4	0.63
PP/SEBS (15%)	122.0	129.0	58.6	6.0	97	7.6	0.62
PP/SEBS (20%)	121.5	128.5	51.0	5.75	96	8.9	0.60

However, the above-stated four diffraction maxima show a peculiar variation of peak heights with blend composition. As the SEBS content of the blend increases, the height of peak at  $2\theta = 17^\circ$  increases, while those of the peaks at  $2\theta = 14^\circ$  and  $21.7^\circ$  decrease and that of the peak at  $2\theta = 18.5^\circ$  remains almost unchanged. Comparison of the diffraction patterns of the two samples of extreme compositions is presented in Figure 5 to illustrate this peculiar variation of peak heights. Other studies may help here to give further information. Some possible causes for this variation of peak heights could be: variation of mean spherulite size or their distribution, deformation at the spherulite boundaries, or any long-range order induced in the structure by the dispersion of SEBS domains in the PP matrix, or formation of mesomorphic smectic phase of PP.

However, a simple superposition of the diffuse scattering pattern of SEBS (also shown in Fig. 5) to the diffraction pattern of PP does not lead to the shape of diffraction pattern identical to that observed for the blends. It may be seen from Figure 5 that the superposition of the scattering patterns of PP and SEBS would lead to increased peak heights of all peaks in a certain region of  $2\theta$ . Moreover, the intensity of the diffuse scattering maximum of SEBS will be much reduced in the blend samples owing to the smaller domains of SEBS dispersed in the scattering volume.

The degree of crystallinity ( $X_c$ ) was calculated from these diffractograms according to the method described for PP in the literature,<sup>12,13</sup> using the expression

$$x_c = \frac{\int_0^\infty s^2 I_{cr}(s) ds}{\int_0^\infty s^2 I(s) ds} \cdot K \quad (1)$$

where  $I_{cr}(s)$  is the coherent intensity concentrated in the crystalline peaks and  $I(s)$  is the total coherent intensity scattered.  $s$  is the scattering vector, expresses as  $s = (2/\lambda) \sin \theta$ .  $K$  is the correction factor, which depends<sup>12,13</sup> on atomic scattering factors and the disorder function. Owing to the uncertainty<sup>12,13</sup> about the value of disorder function, the factor is ignored in these calculation by taking  $K$  as equal to unity. The degree of crystallinity thus evaluated is denoted as the apparent degree of crystallinity,  $(X_c)_{app}$ , which may be emphasized for its comparative value alone.



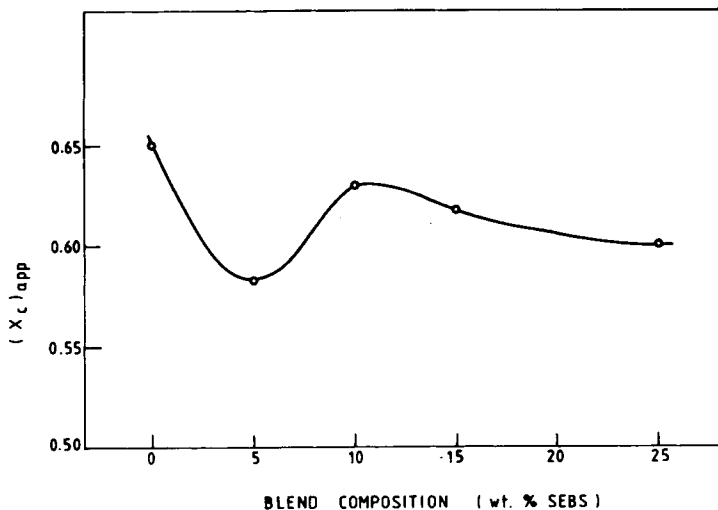


Fig. 7. Variation of X-ray crystallinity with blend composition for PP/SEBS blends.

The experimental  $I$  vs.  $2\theta$  curves were converted into  $Is^2$  vs.  $s$  curves. Amorphous scattering curve and the baseline were drawn in accordance with those shown in Figure 25 of Ref. 12, which were suggested<sup>13</sup> to be more appropriate than those used by other authors.<sup>12</sup> The  $Is^2$  vs.  $s$  curve of unblended PP sample is shown in Figure 6 as a typical illustration of the baseline and the amorphous scattering curve used in these calculations. The resemblance of the  $Is^2$  vs.  $s$  curves of these samples with those reported for isotactic polypropylene by other authors<sup>12,13</sup> is noteworthy.

Crystallinity values ( $X_c$ )<sub>app</sub> thus obtain for the various samples are shown in Table I. Crystallinity varies with SEBS content of the blend in a manner shown in Figure 7. As the SEBS content of the blend increases, the crystallinity of PP first decreases from its value for unblended PP, passes through minimum at 5% SEBS content, then increases for the blend with 10% SEBS content, and thereafter decreases again with increasing SEBS content. The variation of ( $X_c$ )<sub>app</sub> with blend composition is in good qualitative agreement with the variation of crystallinity parameter  $A/m$  in DTA studies (see Fig. 3). Thus, these X-ray diffraction results provide a supporting evidence for the effect, observed in DTA studies, of blending with SEBS on the crystallization of PP.

### Tensile Properties

Results of tensile testing of these PP/SEBS blends are shown in Figure 8, where tensile strength, elongation at break, tensile elastic modulus, yield stress, and yield strain are plotted as functions of blend composition. The data points in this figure represent the mean value while the vertical bars denote the range of experimental values on the several samples tested for each blend composition.

In region 1 of the blend composition (i.e., 0–5% SEBS), tensile strength, modulus, elongation at break, and yield stress decrease, while the yield strain increases. This is the region consistent with the decrease of crystallinity and

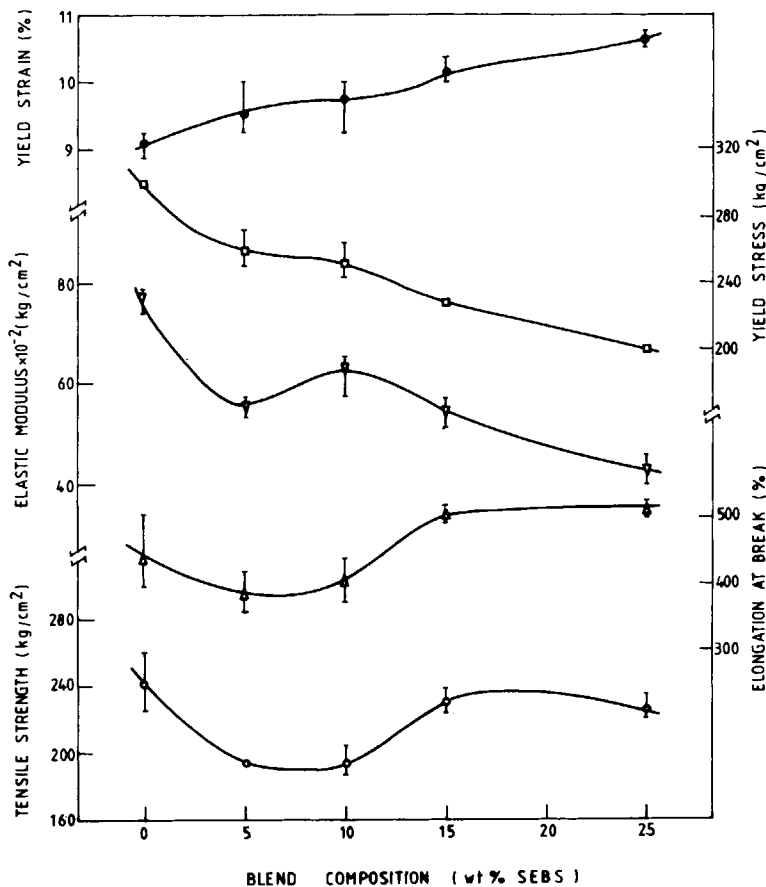


Fig. 8. Tensile properties of PP/SEBS blends as function of blend composition.

the formation of large spherulites (or increase in spherulite size distribution) of PP.

In region 2 of the blend composition (i.e., 5–15% SEBS), tensile strength, elongation at break, and yield strain increase, while yield stress decreases continuously with increasing SEBS content. Modulus, on the other hand, increases up to 10% SEBS content and then decreases at higher SEBS content. This region is consistent with the increase of crystallinity and the formation of small spherulites of PP.

In region 3 of the blend composition (i.e., 15–25% SEBS) tensile strength, modulus, and yield stress decrease, while the elongation at break and yield strain increase with increasing SEBS content. This region is consistent with the formation of large spherulites and decrease of crystallinity of PP.

Values of tensile strength, modulus, and yield stress are lower, while those of the yield strain are higher, for the blends than those for PP, even in region 3 of the blend composition. However, elongation at break is higher for the blend than PP only in region 3 of the blend composition. Decrease of tensile strength, modulus, yield stress, and increase in elongation at break for the blends of PP with other polymers are reported by other authors.<sup>7</sup>

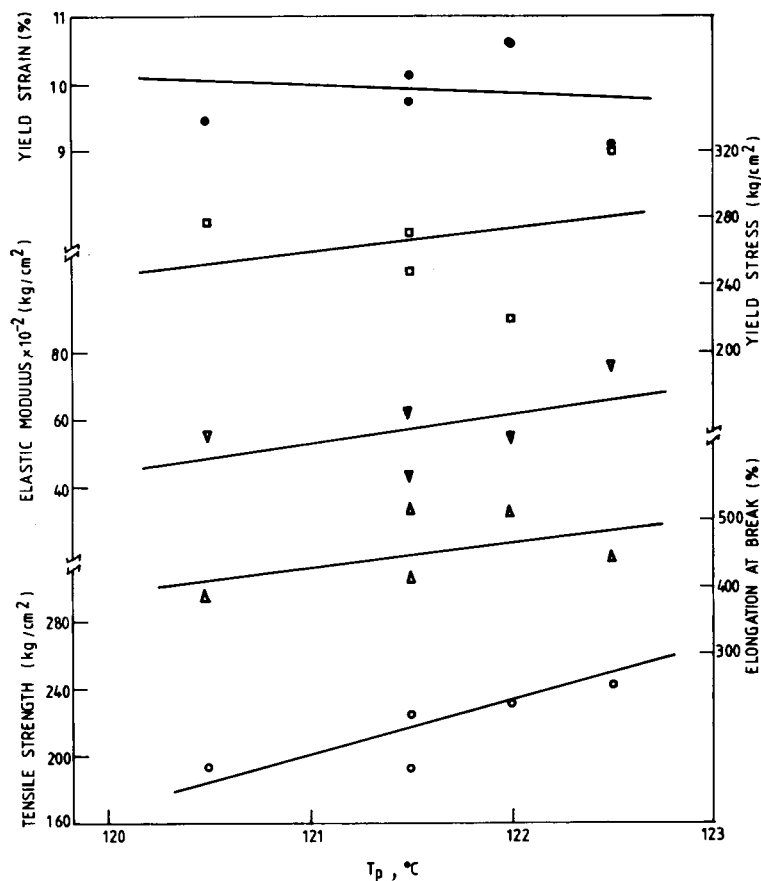


Fig. 9. Correlation of the tensile properties with  $T_p$ .

### Correlation of Mechanical Properties and Crystallization Parameters

Beck and Ledbetter<sup>9</sup> found that the addition of nucleating agents, which increased the nucleation rate and the degree of supercooling as well as the crystallinity, produced a systematic effect on the tensile properties of PP. Variations of tensile strength, modulus, yield stress, and elongation at break with  $T_p$  were found linear with some scatter of the data points. The scatter of data points were attributed to differences in nucleating ability of the nucleating agents and the concentration fluctuations, or presence of impurities, or to particle size differences.<sup>9</sup> We have attempted to find similar correlations of tensile properties of these samples with  $T_p$  and the spherulite size distribution parameter ( $\Delta w$ ), as shown in Figures 9 and 10. For these data in the limited range, the linearity of the correlations was determined through the regression analysis, on the basis of the value of the coefficient of correlation in each individual case. The closer to unity the value of coefficient of correlation, the better the linearity of the fit. Values of coefficient of correlation are shown in Table II for the correlations of the various pairs of these parameters. On the basis of the extremely low values of the coefficient of correlation, linear relationships of some of these pairs of parameters may be rejected straightaway. Finally, allowing some discount to

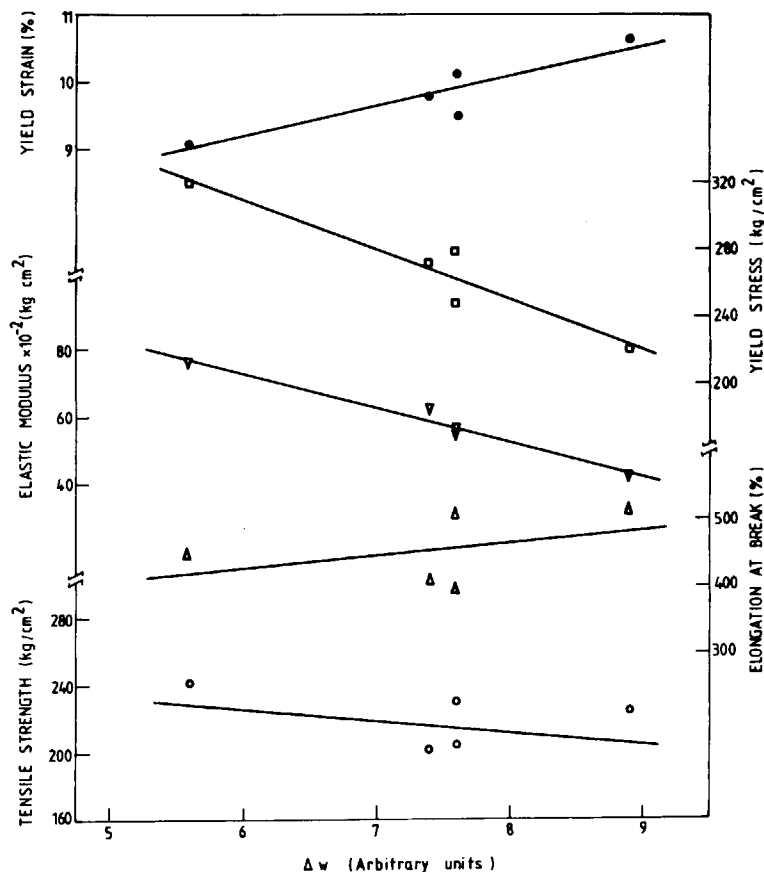


Fig. 10. Correlation of the tensile properties with  $\Delta w$ .

the scatter of the data points due to experimental precision, we may take the correlations with coefficient of correlation greater than 0.7 to represent a good linearity of the correlation. Thus we obtained the following expressions of linear correlations:

$$\sigma_t = 32.36T_p - 3714.8 \quad (2)$$

$$E_m = 10.35\Delta w + 135.2 \quad (3)$$

$$\sigma_y = 30.06\Delta w + 490.8 \quad (4)$$

$$\epsilon_y = 0.45\Delta w + 6.48 \quad (5)$$

where  $\sigma_t$ ,  $E_m$ ,  $\sigma_y$ , and  $\epsilon_y$  represent tensile strength, tensile elastic modulus, yield stress, and yield strain, respectively.

Correlations of  $T_p$  with X-ray and DTA crystallinity parameters  $(X_c)_{app}$  and  $A/m$  are presented in Figure 11. These correlations are sufficiently linear and are in good qualitative agreement with the linear correlation of density with  $T_p$  reported<sup>9</sup> for PP in the presence of nucleating agents. The correlation presented in Figure 11 implies not only the consistency of the DTA and X-ray crystallinities but also suggests a correlation of tensile properties with crystallinity similar to those shown with respect to  $T_p$  in Figure 9.

TABLE II  
Coefficient of Correlation for the Linear Correlation of the Various Parameters

Tensile property	Crystallization parameter	Coefficient of correlation
Tensile strength	$T_p$	0.73
	$\Delta w$	0.11
Tensile elastic modulus	$T_p$	0.27
	$\Delta w$	0.96
Elongation at break	$T_p$	0.23
	$\Delta w$	0.17
Yield stress	$T_p$	0.08
	$\Delta w$	0.91
Yield strain	$T_p$	0.02
	$\Delta w$	0.81

These correlations, shown in Figures 9 and 10 and Table II, suggest that, out of the various tensile properties, the tensile strength is more distinctly related to the crystallinity of PP in the blend. Tensile elastic modulus, yield stress, and yield strain, on the other hand, are more distinctly related to the crystallite size distribution parameter ( $\Delta w$ ). These correlations seem to confirm the effect of the crystallization of PP component on the tensile properties of the blend. However, in the case of those pairs of the parameters where the coefficient of correlation is too low, the correlations might be more complex than the simple linear correlation.

As already stated, the lower values of  $\Delta w$  are consistent with smaller spherulites in the structure. Thus these results may be taken to imply that the modulus and yield stress decrease, while the yield strain increases with increasing size of the PP spherulites in these blends. Increase in yield stress and tensile strength of PP on addition of crystal nucleating agents, and its correlation with decreasing spherulite size is reported in the literature.<sup>14,15</sup> Kuhre et al.<sup>16</sup> found that the crystallinity increase associated with addition of nucleant was important in enhancing the tensile strength. Furthermore, similar correlations of spherulite size (measured through aging characteristics) of PP with varying proportion of nucleating agents with tensile strength and yield stress have been reported by Remaly and Schultz.<sup>17</sup>

In these data on PP/SEBS blends, though, unlike the case of modulus and yield stress, the linearity of correlation of tensile strength with  $\Delta w$  is not apparent over the whole range of blend composition, the increase of tensile strength with decreasing spherulite size, and vice versa, are clearly observed in the regions of 5–10% and 15–25% SEBS contents, respectively.

It may be remarked that the information about the spherulite size obtained from  $\Delta w$  and nucleation rate parameters is quite consistent with the results reported<sup>9</sup> from the measurement of variation of optical clarity with  $T_p$  for PP with nucleating agents. Optical clarity, which is inversely related to the spherulite size, remained independent of  $T_p$  at low  $T_p$  and then increased with increasing  $T_p$  for PP containing nucleating agents.<sup>9</sup> The results in these PP/SEBS blends are somewhat different from those of PP with nucleating agents. However, the presence of larger spherulites at lower  $T_p$  and then a decrease in spherulite size with increasing  $T_p$  is seen in these data in the boundary zone of regions 1 and 2 of the blend composition.

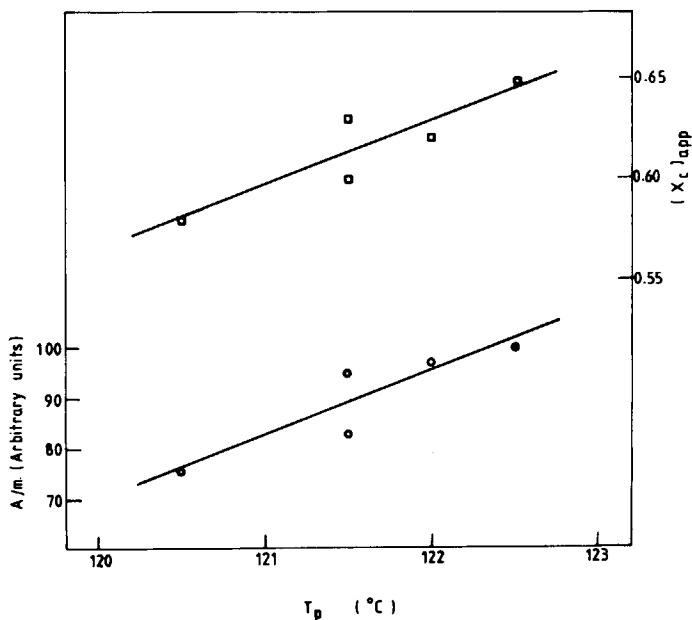


Fig. 11. Correlation of DTA and X-ray crystallinity parameters with  $T_p$ .

## CONCLUSIONS

Crystallization exotherms of PP in the DTA thermograms of PP/SEBS blends provide information about the crystallization behavior of PP component in the blend. The crystallinity determined by area under the exotherm peak is in good qualitative agreement with the X-ray crystallinity. Furthermore, the exotherm peak temperature increased linearly with increasing crystallinity.

In the region of low SEBS content (i.e., 0–5%), the blending induces a decrease in crystallinity, increase in spherulite size accompanied by the decrease in tensile strength, modulus, elongation at break, and yield stress, and the increase in yield strain, with increasing SEBS content. In the intermediate region of SEBS content (i.e., 5–15%) crystallinity increases while the spherulite size is small. Accompanying changes in the tensile properties are such that the tensile strength, modulus, elongation at break, and yield strain increase, while the yield stress decreases with increasing SEBS content. In the region of higher SEBS content (i.e., 15–25%) crystallinity decreases while spherulite size increases, which is accompanied by decrease in tensile strength, modulus, and yield stress and increase in elongation at break and yield strain.

Furthermore, these results reveal distinction of the role of crystallinity and crystallite size distribution on the various tensile properties. Tensile elastic modulus and yield behavior (yield stress and yield strain) are predominantly dependent on the crystallite size distribution, while the tensile strength is predominantly dependent on the crystallinity. This suggests that the crystallization of PP component influences the tensile properties of PP/SEBS blends.

## References

1. A. K. Gupta, V. B. Gupta, R. H. Peters, W. G. Harland, and J. P. Berry, *J. Appl. Polym. Sci.*, **27**, 4669 (1982).

2. A. P. Plochocki, in *Polymer Blends*, D. R. Paul and S. Newman, Eds., Academic, New York, 1978, Vol. 2.
3. C. D. Han, *Rheology in Polymer Processing*, Academic, New York, 1976.
4. C. Markin and H. L. Williams, *J. Appl. Polym. Sci.*, **25**, 2451 (1980).
5. F. C. Stehling, T. Huff, C. S. Spead, and G. Wissler, *J. Appl. Polym. Sci.*, **26**, 2693 (1981).
6. D. L. Siegfried, D. A. Thomas, and L. H. Sperling, *J. Appl. Polym. Sci.*, **26**, 177 (1981).
7. C. R. Lindsey, D. R. Paul, and J. H. Barlow, *J. Appl. Polym. Sci.*, **26**, 177 (1981).
8. A. K. Gupta and S. N. Purwar, *J. Appl. Polym. Sci.*, **29**, 1079 (1984).
9. H. N. Beck and H. D. Ledbetter, *J. Appl. Polym. Sci.*, **9**, 2131 (1965).
10. F. Rybnikar, *J. Appl. Polym. Sci.*, **27**, 1479 (1982).
11. G. Natta and P. Corradini, *Nuovo Cimento (Suppl.)*, **15**, 40 (1960).
12. W. Ruland, *Acta Crystallogr.*, **14**, 1180 (1961).
13. M. Sotton, A. M. Arniaud, and C. Rabourdin, *Bull. Sci. Inst. Text. Fr.*, **7**, 265 (1978).
14. V. A. Kargin, *Russ. Chem. Rev. (Engl. transl.)*, **35**, 427 (1966).
15. T. I. Sogolova, *Polym. Mechn.*, **1**, 1 (1965).
16. C. J. Kuhre, M. Wales, and M. E. Doyle, *Soc. Plast. Eng. J.*, **20**, 1113 (1964).
17. L. S. Remaly and J. M. Schultz, *J. Appl. Polym. Sci.*, **14**, 871 (1970).

Received July 22, 1983

Accepted October 5, 1983